COMPUTER MODELLING OF METAL-SEMICONDUCTOR JUNCTIONS

F. MASSZI

Department of Electron Devices,
Technical University, H-1521 Budapest

Summary

The paper presents the Program M—S junction for simulating metal-semiconductor (Schottky) junctions. The used algorithm is that of the Program P—N junction's with the completion of the appropriate boundary conditions and some minor changes. Both the diffusion and the combined thermionic-emission-diffusion models for the metal-semiconductor junctions have been used to obtain one-dimensional, numerical two carrier solutions, for silicon Schottky-diode structures. The methods for calculating diode capacitance are also discussed. Results are compared with fabricated silicon Schottky-diodes.

Introduction

The paper presents the Program M—S [1] for simulating metal-semiconductor (Schottky) junctions. The used algorithm is that of the Program P—N junction's [2] with the completion of the appropriate boundary conditions and some minor changes. Both the diffusion and the combined thermionic-emission-diffusion models for the metal-semiconductor junctions have been used to obtain one-dimensional, numerical two-carrier solutions, for silicon Schottky-diode structures. The methods for calculating Schottky-diode capacitance are also discussed. Standard methods for determining structure parameters, mostly barrier height, have been applied to the numerical results. The results have also been compared with fabricated silicon Schottky-diodes.

Basic equations

The used physical model is based on the well-known partial differential equation system of semiconductors. This system of equations consists of the transport equations:

$$\bar{J}_n = q\mu_n n\bar{E} + qD_n \operatorname{grad} n \tag{1}$$

$$\bar{J}_p = q\mu_p p\bar{E} - qD_p \operatorname{grad} p \tag{2}$$

of the continuity equations:

$$\frac{\partial n}{\partial t} = U + \frac{1}{q} \operatorname{div} \bar{J}_n \tag{3}$$

$$\frac{\partial p}{\partial t} = U - \frac{1}{q} \operatorname{div} \bar{J}_p \tag{4}$$

of the Poisson-equation:

$$\operatorname{div} \operatorname{grad} \Psi = \frac{q}{\varepsilon} (n - p - N) \tag{5}$$

and of the current equation:

$$\bar{J} = \bar{J}_n + \bar{J}_p + \varepsilon \frac{d\bar{E}}{dt} \tag{6}$$

where the symbols have their usual meanings:

n, p: carrier concentrations of electrons and holes, respectively,
μ_n, μ_p: mobilities of electron and hole carriers, respectively,
$\bar{J}_n$, $\bar{J}_p$: electron and hole current densities, respectively,
D_n, D_p: diffusion coefficients of electron and hole carriers, respectively,
q: electron charge ($1{,}602 \cdot 10^{-19}$ As),
E: electric field-strength,
Ψ: electric potential,
U: net generation-recombination rate,
N: net impurity concentration,
t: time,
ε: dielectric constant.

The equations are transformed to one-dimensional D. C. state and normalized after de Mari [3]:

$$J_n = \mu_n \left(n \frac{d\Psi}{dx} - \frac{dn}{dx} \right) \tag{7}$$

$$J_p = \mu_p \left(p \frac{d\Psi}{dx} + \frac{dp}{dx} \right) \tag{8}$$

$$\frac{dJ_n}{dx} - U = 0 \tag{9}$$

$$\frac{dJ_p}{dx} + U = 0 \tag{10}$$

$$\frac{d^2\Psi}{dx^2}=n-p-N \tag{11}$$

$$J=J_n+J_p \tag{12}$$

Table I

Normalization factors

Description	Normalized quantity	Normalization factors		
		Symbol	Value in Si	Unit
Position (length)	x	$L_D=\sqrt{\frac{\varepsilon_0\varepsilon_r V_T}{qN_i}}$	3.45706E−03	cm
Time	t	t_0	1.19513E−05	sec
Potential	Ψ, V, V_D etc.	$V_T=\frac{kT}{q}$	2.58750E−02	volt
Current density	J, J_n, J_p	$J_0=\frac{qD_0n_i}{L_D}$	−6.71929E−07	$\frac{\text{amper}}{\text{cm}^2}$
Carrier density	n, p, $N_D^+ \cdot N_A^-$	n_i	1.45000E+10	cm^{-3}
Mobility	μ_n, μ_p	$\mu_0=\frac{D_0}{V_T}$	3.86473E+01	$\frac{\text{cm}^2}{\text{Vsec}}$
Diffusivity	D_n, D_p	D_0	1.0	$\frac{\text{cm}^2}{\text{sec}}$
Velocity	s_n, s_p	$s_0=\frac{D_0}{L_D}$	2.89263E+02	$\frac{\text{cm}}{\text{sec}}$

For the normalization factors see Table 1. Solution is made according to the Gummel—de Mari—Tarnay method [4], [3], [2], while generation-recombination rates a calculated form the simple Schottky—Read—Hall model [5], [6]

$$U=\frac{np-n_i^2}{\tau(n+n_1)+\tau(p+p_1)} \tag{13}$$

Mobility calculations are based on Caughey's and Thomas's model [7]

$$\mu_p=47,7+\frac{447,3}{1+\left(\frac{\text{N}[\text{cm}^{-3}]}{6,3\cdot 10^{16}}\right)^{0.76}}\left[\frac{\text{cm}^2}{\text{Vsec}}\right] \tag{14}$$

$$\mu_n = 65 + \frac{1265}{1 + \left(\frac{\mathrm{N[cm^{-3}]}}{8{,}5 \cdot 10^{16}}\right)^{0{,}72}} \left[\frac{\mathrm{cm^2}}{\mathrm{Vsec}}\right] \tag{15}$$

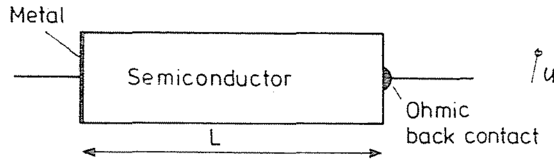

Fig. 1. M—S (Schottky) diode in one dimension

The input of the algorithm: geometric data, doping profile, and the boundary conditions describing the contacts. Output: electron and hole carrier distributions, potential distributions vs. position and low-level I—V characteristics both in forward and reverse directions.

Boundary conditions

Ohmic contact

Ohmic contact is assumed at the back of the diodes. Supposing infinite surface recombination velocities the charge neutrality,

$$\rho = q(p - n + N) = 0 \tag{16}$$

and the law of mass effect,

$$np = n_i^2 \tag{17}$$

are valid, where

ρ: charge density,
n_i: intrinsic carrier concentration ($\approx 1{,}4 \cdot 10^{10}/\mathrm{cm}^3$).

Quadratic solutions form the above two equations,

$$n = \frac{N}{2} + \sqrt{\frac{N^2}{4} + n_i^2} \tag{18}$$

$$p = -\frac{N}{2} + \sqrt{\frac{N^2}{4} + n_i^2} \tag{19}$$

give the possibility for calculating the $n(L)$, $p(L)$ boundary conditions for both carrier concentrations at the back contact.

As for potential, two different cases are to be distinguished:

a) zero applied voltage on diode.

Then

$$\Psi(0)=0 \tag{20}$$
$$\Psi(L)=-V_D \tag{21}$$

where

$$V_D=U_T \ln \frac{n(0)}{n(L)} \tag{22}$$

is the diffusion (built-in) potential in the diode (Boltzmann approximation), and

$$V_T = \text{thermal potential } (\approx 26\ \text{mV at } 300\ ^\circ\text{K})$$

b) In case of $V_A \neq 0$

$$\Psi(0)=0 \tag{23}$$
$$\Psi(L)=-V_D-V_A \tag{24}$$

where V_A: applied voltage on diode.

Diffusion model

The assumption made in the diffusion theory is that the concentration of the carriers on the semiconductor side of the M—S junction interface is unaltered by the application of bias. This is equivalent to assuming that at the interface the quasi-Fermi-levels in the semiconductor coincide with the Fermi-level in the metal. It means that the electron quasi-Fermi-level drops through the depletion region as shown (Fig. 2 and 3).

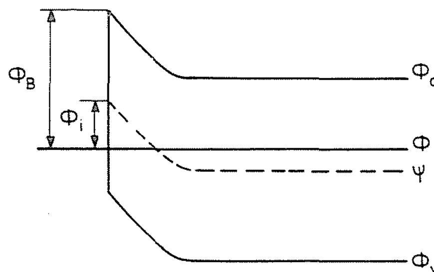

Fig. 2. Band diagram of an M—S junction with zero applied voltage

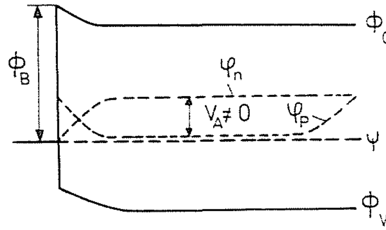

Fig. 3. Band diagram of forward biased M—S junction assuming diffusion model at the M—S boundary

This behaviour is in sharp contrast with the situation in a p—n junction under bias, where the quasi-Fermi-levels for both type of carriers are generally assumed to be flat throughout the depletion region. In other words, the diffusion theory assumes the validity of the law of the mass effect,

$$np = n_i^2 \tag{17}$$

just at the interface (but not in the depletion region considering the exact surface as it is not part of the depletion region). That means: infinite recombination velocity is assumed.

Carrier concentrations at the M—S junction can be calculated on the basis of the diffusion model:

$$n(0) = n_i e^{\frac{\Phi_i}{U_T}} \tag{25}$$

$$p(0) = p_i e^{-\frac{\Phi_i}{U_T}} \tag{26}$$

where

$$\Phi_i = \Psi - \Phi = \frac{U_g}{2} - \Phi_B \tag{27}$$

is the difference between the electrostatic and Fermi potential, and

Ψ: electrostatic potential,
Φ: Fermi potential,
U_g: band gap,
Φ_B: barrier height.

Image force lowering of the barrier

When an electron approaches a metal, the requirement that the electric field must be perpendicular to the surface enables the electric field to be calculated as if there was a positive charge of magnitude q located at the mirror image of the electron with respect to the surface of the metal. There is a Coulomb-force due to this the electron has a negative potential energy relative to that of an electron at infinity. The image potential energy has to be added to the potential energy due to the Schottky barrier. Since the image potential is only important near the surface, it is a very good approximation as regards the field due to the Schottky barrier as constant with the value E_{max}.

This effect is present only if there is an electron present in the conduction band near the top of the barrier. On the other hand, contributions to the barrier height from work function difference and from surface states are present whether or not there is an electron. Holes are attracted to the metal by an image force, too. Their energy is measured downwards, so the band bends upwards (not uniform bandgap) Fig. 4.

If the effect of image force lowering is included, Eqs (25) and (26) are slightly modified:

$$n(0)=n_i e^{\frac{\Phi_i+\Delta\Phi_B}{U_T}} \tag{28}$$

$$p(0)=n_i e^{-\frac{\Phi_i-\Delta\Phi_B}{U_T}} \tag{29}$$

where

$$\Delta\Phi_B=\sqrt{\frac{q\cdot E_{max}}{4\pi\varepsilon}} \tag{30}$$

is the barrier lowering.

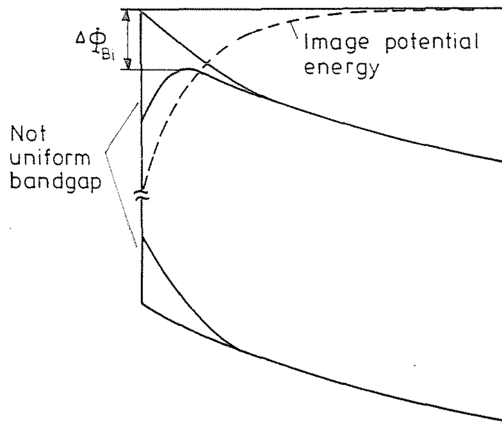

Fig. 4. The effect of image force lowering on the bandgap of the M—S junction

Thermionic-emission model

This model assumes that the current limiting process is the actual transfer of electrons across the metal-semiconductor interface. This is mostly equivalent with the well-known very simple one-carrier model, where the I—V characteristics are given by

$$I = A^* T^2 e^{-\frac{\Phi_B}{U_T}} \cdot \left(e^{\frac{V_A}{U_T}} - 1\right) \tag{31}$$

where

A^*: Richardson-constant,
T: (absolute) temperature,
and the other symbols have already been defined.

According to the thermionic-emission model the effect of drift and diffusion in the depletion region is assumed to be negligible that means the φ_n and φ_p quasi-Fermi levels are flat in the depletion region, consequently $\varphi_n(0)$ and $\varphi_p(0)$ do not coincide at the metal-semiconductor interface (Fig. 5):

$$n(0) = n_i e^{\frac{\Phi_i - V_A}{U_T}} \tag{32}$$

$$p(0) = p_i e^{-\frac{\Phi_i}{U_T}} \tag{33}$$

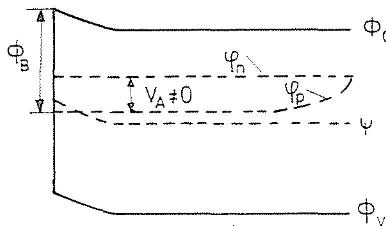

Fig. 5. Band diagram of forward biased M—S junction assuming thermionic-emission model at the M—S boundary

The combined model

Several authors have combined the thermionic-emission and diffusion theories by considering the two mechanisms to be in series and effectively finding the position of the quasi-Fermi levels at the interface equalizing the current flowing through each of them. The most developed theory is that of Crowell and Sze [8] who introduced the concept of a recombination velocity (2) at the top of the barrier, and determined the current density as

$$J = s[n(0) - n_0] \tag{34}$$

where n_0 is the equilibrium electron concentration with infinite s, and $n(0)$ is the actual concentration of electrons (Fig. 6):

It is noted that previous models first determined the position of Fermi-levels, and derived carrier concentrations based upon the position of the Fermi-levels. In the combined diffusion-thermionic-emission model carrier concentrations are to be determined first, and the Fermi-level is calculated thereafter.

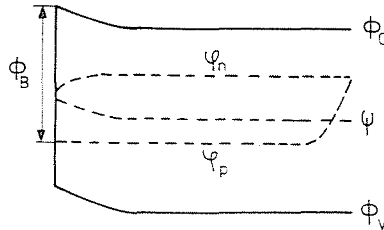

Fig. 6. Band diagram of forward biased M—S junction assuming combined diffusion-thermionic-emission model at the M—S boundary

The algorithm is as follows:

1. Calculate the equilibrium concentrations n_0 and p_0 from the diffusion model (image force lowering effect included) according to Eqs (25)—(30).
2. Set a system of equations with four unknowns as follows:

$$J_n(0) = s_n[n(0) - n_0] \tag{35}$$
$$J_p(0) = s_p[p(0) - p_0] \tag{36}$$
$$J_n(0) = f[n(0), \dots] \tag{37}$$
$$J_p(0) = f[p(0), \dots] \tag{38}$$

   The first two equations represent the combined model, the second two come from the Gummel—de Mari—Tarnay algorithm (see Appendix).
3. Solve system of equations (35)—(38) for $J_n(0)$, $J_p(0)$, $n(0)$ and $p(0)$.

The capacitance of a Schottky-diode

Consider the ideal Schottky diode (with no interfacial layer between the metal and semiconductor). Let us change the reverse applied voltage V_R to $V_R + \Delta V_R$. As a consequence

— electrons recede further from the metal,

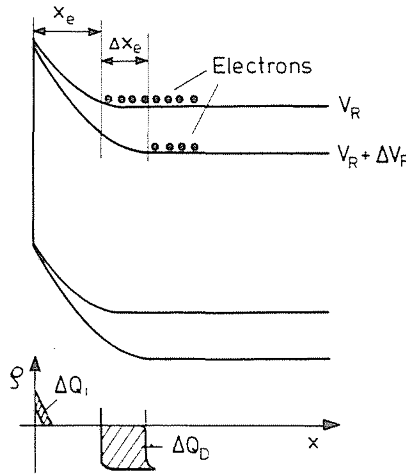

Fig. 7. Band diagram of reverse biased M—S junction (V_R: reverse voltage, x_e: width of depletion layer, Q_I and Q_D: charges in the inversion and depletion layers, respectively)

— hole concentration in the inversion layer decreases because the hole-quasi-Fermi-level coincides with the metal Fermi-level.

The change in the charges gives rise to a capacitance. There are three types of charges. Which of them is to be taken into account? The question can be solved by considering the various contributions to the current density through the depletion region.

$$J = J_{c1} + J_{c2} + \varepsilon \frac{dE}{dt} \tag{39}$$

where

J_{c1} is due to the drift and diffusion of electrons injected over the barrier from the metal,

J_{c2} arises because there is a flow of electrons and holes out of the depletion region as the negative bias increases.

It can be assumed that in the depleted region

$$Q_D \cong q \cdot N_D \neq f(t) \tag{40}$$

where N_D is the ionized dopant density concentration in the depletion layer.

Consequently, the capacitive current consists of displacement current

$$J = C \frac{dV_R}{dt} = \varepsilon_s \frac{dE}{dt} = \varepsilon_s \frac{dE}{dV_R} \cdot \frac{dV_R}{dt} \tag{41}$$

where ε_s is the permittivity of the semiconductor. According to Gauss' theorem

$$\varepsilon_s \Delta E = \Delta Q_D \tag{42}$$

and from here

$$C = \frac{\Delta Q_D}{\Delta V_R} = -\frac{\partial(Q_m + Q_i)}{\partial V_R} \tag{43}$$

where
Q_D: charge in the depletion region,
Q_m: metal charge,
Q_i: charge in the inversion region,
and

$$Q_D + Q_m + Q_i = 0 \tag{44}$$

In computer modelling, basically two ways are used to calculate the capacitance:
1. integration of the charge carrier distribution in order to get the charge to be differentiated,
2. calculation of the
   a) electrically stored energy,
   b) total thermodynamically stored energy.

Let us see these two methods in details.

Method of the integration of charge carrier distributions

The essence of the method is to evaluate the following integral

$$C = q \int_0^L \frac{\partial n}{\partial V} dx \tag{45}$$

(in case of n-type semiconductors).

The numerical evaluation is prone to error, unless many significant digits can be obtained in the numerical solutions for the electron densities. This requirement places extensive demands on an already difficult numerical problem. Roundoff errors may easily overshadow the important changes in charge density that occur at the edges of the depletion region.

The usual way of calculation [9]

$$C=q\int_0^L \frac{\partial n}{\partial V}dx=q\frac{d}{dV}\int_0^\xi ndx+q\frac{d}{dV}\int_\xi^L ndx \tag{46}$$

The operation of differentiation with respect to voltage may be taken outside of the integral since both 0 and L are fixed points. Furthermore, the interval $[0, L]$ may be broken into two parts by selecting a point ξ interior to the interval. In doing this, one should observe, that the value of C is independent of the manner in which ξ is chosen. In general, ξ will depend upon V for its value:

$$\xi=\xi(V) \tag{47}$$

$\xi(V)$ can be e.g. $=X_e$, the depletion region boundary.

Each of the integrals is then evaluated by Leibniz's theorem:

$$\frac{d}{dV}\int_0^{\xi(V)} n(x,V)\,dx=\lim_{\Delta V\to 0}\frac{\int_0^{\xi(V+\Delta V)} n(x,V+\Delta V)\,dx-\int_0^{\xi(V)} n(x,V)\,dx}{\Delta V}=$$

$$=\lim_{\Delta V\to 0}\int_0^{\xi(V)}\frac{n(x,V+\Delta V)-n(x,V)}{\Delta V}dx+ \tag{48}$$

$$+\lim_{\Delta V\to 0}\int_{\xi(V)}^{\xi(V+\Delta V)}\frac{n(x,V+\Delta V)}{\Delta V}dx$$

The upper limit of the first integral $\xi(V)$ may be replaced with the specific point X_e. The integrand of the second integral as a limit tends to $n(X_e, V)$ which may be removed from the integral. Thus taking the limit yields the following equation:

$$\frac{d}{dV}\int_0^{\xi(V)} n(x,V)\,dx=\int_0^{X_e}\frac{\partial n(x,V)}{dV}dx+n(X_e,V)\frac{d\xi(V)}{dV} \tag{49}$$

We must choose X_e that both of the integrals have to be evaluated of relatively small dynamic range of the variables. The evaluation goes with a numerical Newton—Cotes formula.

The energetic way of calculation

a) Electrically stored energy.

A philosophically sound method should relate capacitance to some fundamental circuit property. One might compute incremental capacitance by computing the total change in stored energy that results from a change in applied terminal voltage.

$$\Delta W = \frac{1}{2} C(V + \Delta V)^2 - \frac{1}{2} CV^2 \tag{50}$$

If $V \neq 0$ and ΔV is small enough so that C remains reasonably constant over ΔV,

$$C = \frac{1}{V} \frac{\Delta W}{\Delta V} \tag{51}$$

In fact the result of this is different from the results of the previous calculation, because the total stored energy is not the same as the energy stored in the electrostatic field! The most obvious difference occurs in a junction at thermodynamic equilibrium in which by definition, there is no available stored energy, although an electric field exists.

b) Thermodynamically stored energy

Thermodynamically the energy W (in eV) added to a system by a process of adding Δn particles to a point in the system where each particle has an electrochemical potential of μ eV is given

$$W = \mu \, \Delta n \tag{52}$$

Implicitely the process means the transport of a particle from a place where the potential energy is zero: i.e. from a point well removed from the system, to the point in question.

In a semiconductor the particles consist of electrons and holes. In the followings the hole is regarded as an equivalent particle. If electrons are moved from an outside point to a point within the semiconductor where they will have μ_n [eV] electrochemical potential, then μ^n [eV] of energy is added to the system. The situation is just the same in the case of the holes, with μ^p [eV] of energy.

If both electrons and holes in respective quantities of Δn and Δp are added with the respective electrochemical potentials of μ^n and μ^p, the net energy, if the change in the carrier densities is small

$$\Delta W = \mu^n \, \Delta n + \mu^p \, \Delta p \tag{53}$$

Because all are function of x

$$\Delta W = \int_0^L (\mu^n \Delta n + \mu^p \Delta p)\, dx \tag{54}$$

Moreover, if the changes in the electron and hole populations occur in response to a change in terminal voltage ΔV that is applied between the ends of the device, the derivative of energy added with respect to applied voltage may be expressed as

$$\frac{dW}{dV} = \int_0^L \left(\mu^n \frac{\partial n}{\partial V} + \mu^p \frac{\partial p}{\partial V}\right) dx \tag{55}$$

An electrochemical potential consists of two independent parts:

$$\mu^n = \underbrace{-q\,\Psi(x)}_{\text{electrostatic energy results from an electric field of an electron at } x} + \underbrace{q\Phi^n(x)}_{\text{chemical energy of an electron at } x} \tag{56}$$

The formula is the same for holes:

$$\mu^p = q\,\Psi(x) + q\,\Phi^p(x) \tag{57}$$

The electrical potential $\Psi(x)$ is related, in a conventional manner, to electrostatic field theory. The chemical potentials are related to the statistics of n and p within the semiconductor.

Under the assumption that the semiconductor is nondegenerately doped so that the Maxwell—Boltzmann statistics apply:

$$\Phi^n(x) = U_T \ln\left(\frac{n}{n_i}\right) \tag{58}$$

$$\Phi^p(x) = U_T \ln\left(\frac{p}{n_i}\right) \tag{59}$$

At this point, the derivative with respect to V of energy added to a semiconductor may be shown to consist of two components: the derivatives with respect to V of energy added to the electrical and chemical fields. Thus

$$\frac{dW}{dV}=\underbrace{\int_0^L q\,\Psi(x)\cdot\left(\frac{\partial p}{\partial V}-\frac{\partial n}{\partial V}\right)dx}_{}+\int_0^L q\left(\Phi^n\frac{\partial n}{\partial V}+\Phi^p\frac{\partial p}{\partial V}\right)dx \tag{60}$$

This occurs when only the electrical field is taken into consideration.

The incremental capacitance may therefore be expressed by

$$C=\frac{1}{V}\begin{pmatrix}\text{The rate of change}\\ \text{with energy } V \text{ added}\\ \text{to the electric field}\end{pmatrix}+\frac{1}{V}\begin{pmatrix}\text{The rate of change}\\ \text{with energy } V \text{ added}\\ \text{to the chemical field}\end{pmatrix} \tag{61}$$

$$\downarrow \qquad\qquad\qquad\qquad \downarrow$$

$$\frac{\Delta W^{\Psi}}{\Delta V} \qquad\qquad\qquad\qquad \frac{\Delta W^{\Phi}}{\Delta V}$$

How can the calculation proceed? [10]

As

$$\int_0^L q\Psi\frac{\partial\rho}{\partial V}=\frac{d}{dV}\left(\frac{\varepsilon_0\varepsilon_r}{2}\int_0^L E^2\,dx\right) \tag{62}$$

so

$$\frac{dW}{dV}=\frac{d}{dV}\left(\frac{\varepsilon_0\varepsilon_r}{2}\int_0^L E^2\,dx\right)+kT\int_0^L\left[\ln\left(\frac{P}{n_i}\right)\frac{\partial p}{\partial V}+\ln\left(\frac{n}{n_i}\right)\frac{\partial n}{\partial V}\right]dx \tag{63}$$

and with

$$\frac{d}{dx}(y\ln y-y)=\ln y\frac{dy}{dx} \tag{64}$$

Eq. (63) can be written as

$$\frac{dW}{dV}=\frac{d}{dW}\left(\frac{\varepsilon_0\varepsilon_r}{2}\int_0^L E^2\,dx\right)+$$

$$+\,kT\frac{d}{dV}\left\{\int_0^L\left[p\ln\left(\frac{p}{n_i}\right)-p+n\ln\left(\frac{n}{n_i}\right)-n\right]dx\right\} \tag{65}$$

The available energy W may be computed by integrating both sides of Eq. (65). In order the available energy shall be equal to zero at $V=0$, the integration constant is taken as the negative of the sum of the electrically and chemically stored energies at $V=0$.

The result can be exposed as follows:

$$W=(W^{\Psi(V)}-W^{\Psi(0)})+(W^{\Phi(V)}-W^{\Phi(0)}) \tag{66}$$

So

$$W=\frac{\varepsilon_0\varepsilon_r}{2}\int_0^L (E^2-E_0^2)\,dx+kT\int_0^L\left[\ln\left(\frac{p}{p_0}\right)\frac{\partial p}{\partial V}+\ln\left(\frac{n}{n_0}\right)\frac{\partial n}{\partial V}\right]dx \tag{67}$$

From here

$$C=\frac{1}{V}\frac{d}{dV}\left(\frac{\varepsilon_0\varepsilon_r}{2}\int_0^L E^2\,dx\right)+\frac{1}{V}\frac{d}{dV}\left\{kT\int_0^L\left[p\ln\left(\frac{p}{n_i}\right)-p+\right.\right.$$

$$\left.\left.+n\ln\left(\frac{n}{n_i}\right)-n\right]dx\right\} \tag{68}$$

Results

Comparison of the diffusion and thermionic-emission-diffusion models has been made in detail elsewhere [11].

Capacitance curves

$C-V$ measurements are used extensively for deducing diffusion potentials (and thus barrier height) and have been considered to be of high reliability. We show in Fig. 8 the $1/C^2-V$ plot for a $\Phi_B=0.80$ ($N_D=5\cdot10^{15}$ cm^{-3}) diode, as calculated from the two-carrier combined model. Capacitance calculations were based on the integration method [9]. A least square fitting of the curve is plotted and in the voltage region of -0.1—0.5 V gives a slope corresponding to a dopant concentration of $N_D=4.97\cdot10^{15}$ 1/cm^3 and a voltage intercept which gives a barrier height of 0.7967 using the estimated value of N_D.

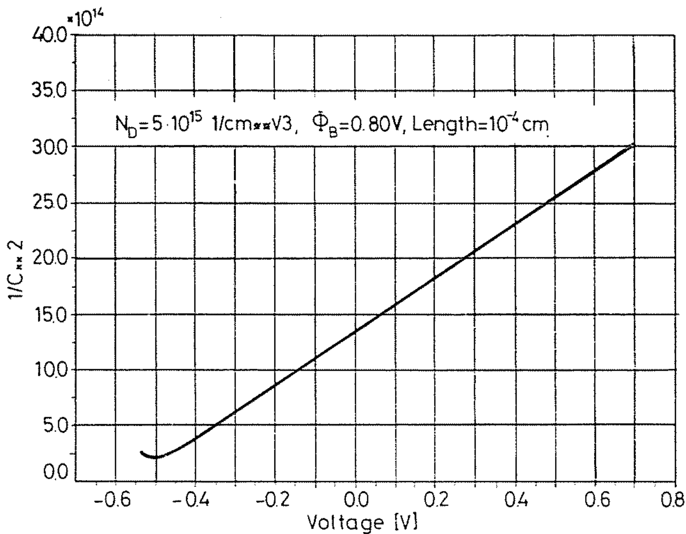

Fig. 8. Computer-plot of $1/C^2$ curve fitting of computed results

I—V characteristics

Determinations of Φ_B for three experimental structures fabricated on materials of different resistivity are compared by the following two methods:

1. extrapolation of forward ln I vs. V plot to determine I_s, and
2. Norde plot [12], also using forward characteristics.

The results are summarized in Table II. It is seen that the $F(V)$ plot determination gives appreciably smaller spread than I—V extrapolations, which also tend to give lower values of Φ_B. This shows the influence of recombination current which is a particularly important contribution to the current in the low voltage region and tends to give too high value for the extrapolated saturation current, thus giving too low barrier heights. The $F(V)$ plot, on the other hand, in essence determines Φ_B from a higher-voltage region of the forward I—V data where recombination current is less important. The difference between the barrier heights determined from calculated and experimental I—V data is approximately 0.02 eV for all diodes using the $F(V)$ [12] method. This shows that the combined model gives results similar to those determined experimentally, although the proper barrier to use in the computer program should be 0.02 eV less than 0.87 eV which was used. I—V extrapolation is very sensitive to recombination current and series resistance to be also seen in Table II.

Table II

Barrier heights determined by forward I—V extrapolation and Norde-plot from I—V data from experimental PtSi—Si diodes and calculated I—V data for similar structures using $\Phi_B = 0.87$ eV in the combined thermionic emission-diffusion model

Resistivity	Experiment		Calculated		Difference	
	I—V	F—V	I—V	F—V	I—V	F—V
6–9 Ω–cm (10 µm epi)	0.84	0.863	0.87	0.877	0.03	0.014
300 Ω–cm (700 µm)	0.81	0.880	0.89	0.900	0.08	0.020
10 K Ω–cm (400 µm)	0.80	0.871	0.83	0.890	0.03	0.019

Barrier height determination from I/C^2 plots gives good results if extrapolated in the low reserve voltage region. However, for the high barrier diode, the barrier found is on the low side.

Our experimental work indicates that extrapolation in the high reserve bias region gives too high barrier values for very high barrier diodes.

Acknowledgement

The author is very grateful to Prof. K. Tarnay, Head of the Department of Electron Devices, Technical University, Budapest and to Prof. P. A. Tove, Head of the Department of Electronics, Uppsala University for their help and valuable support. This work was mostly done at Uppsala University.

Appendix

Derivation of Eqs (37) and (38) from the basic equations is the following:

The transport equations can be rearranged, and treated as two independent first-order linear differential equations in the unknowns n and p, respectively, if the other quantities are considered as non-constant coefficients.

$$\frac{dn}{dx} + n \cdot E = -\frac{J_n}{\mu_n} \tag{A.1.}$$

$$\frac{dp}{dx} - p \cdot E = \frac{J_p}{\mu_p} \tag{A.2.}$$

Analytical solutions are straightforward:

$$n = e^{-\int E dx} \cdot \left[-\int \frac{J_n}{\mu_n} e^{\int E dx} dx + C_n \right] \tag{A.3.}$$

$$p = e^{\int E dx} \cdot \left[\int \frac{J_p}{\mu_p} e^{-\int E dx} dx + C_p \right] \quad (A.4.)$$

Choose 0 and x as limits of integration:

$$n = e^{\Psi} \cdot \left[- \int_0^x \frac{J_n}{\mu_n} e^{-\Psi} dx + C_n \right] \quad (A.5.)$$

$$p = e^{-\Psi} \cdot \left[\int_0^x \frac{J_p}{\mu_p} e^{\Psi} dx + C_p \right] \quad (A.6.)$$

If $x=0$, the integrals are equal to zero, so the constants C_n and C_p can be expressed in terms of $x=0$ boundary conditions,

$$C_n = n(0) e^{-\Psi(0)} \quad (A.7.)$$

$$C_p = p(0) e^{\Psi(0)} \quad (A.8.)$$

and put into (A.5) and (A.6):

$$n = e^{\Psi} \left[n(0) e^{-\Psi(0)} - \int_0^x \frac{J_n}{\mu_n} e^{-\Psi} dx \right] \quad (A.9.)$$

$$p = e^{-\Psi} \left[p(0) e^{\Psi(0)} + \int_0^x \frac{J_p}{\mu_p} e^{\Psi} dx \right] \quad (A.10.)$$

Currents J_n and J_p come from the continuity equations:

$$J_n = \int_0^x U dx + J_{no} \quad (A.11.)$$

$$J_p = - \int_0^x U dx + J_{po} \quad (A.12.)$$

Now put these expressions into (A.9) and (A.10), assuming the boundary conditions at $x=L$ in order to get J_{no} and J_{po}:

$$n(L) = e^{\Psi(L)} \cdot \left[- \int_0^L \frac{e^{-\Psi}}{\mu_n} \cdot \left(- \int_0^x U dx \right) dx - \int_0^L \frac{e^{-\Psi}}{\mu_n} dx \cdot J_{no} + n(0) e^{-\Psi(0)} \right] \quad (A.13.)$$

$$p(L)=e^{-\Psi(L)}\left[\int_0^L \frac{e^{\Psi}}{\mu_p}\left(\int_0^x U dx\right)dx+\int_0^L \frac{e^{\Psi}}{\mu_p}dx\cdot J_{p_0}+p(0)e^{\Psi(0)}\right] \quad \text{(A.14.)}$$

From here

$$J_{n_0}=\frac{n(0)e^{-\Psi(0)}-n(L)e^{-\Psi(L)}+\int_0^L \frac{e^{-\Psi}}{\mu_n}\left(\int_0^x U dx\right)dx}{\int_0^L \frac{e^{-\Psi}}{\mu_n}dx} \quad \text{(A.15.)}$$

$$J_{p_0}=\frac{p(L)e^{\Psi(L)}-p(0)e^{\Psi(0)}-\int_0^L \frac{e^{\Psi}}{\mu_p}\left(\int_0^x U dx\right)dx}{\int_0^L \frac{e^{\Psi}}{\mu_p}dx} \quad \text{(A.16.)}$$

These two equations are to be used instead of Eqs (37) and (38).

References

1. MASSZI, F.: Two-carrier numerical solutions to metal-semiconductor junctions. Uppsala University Institute of Technology reports, UPTEC 8027 R (1980).
2. TARNAY, K.: The Program P—N Junction. Uppsala University Institute of Technology reports, UPTEC 74 78 R (1974).
3. DE MARI, A.: An accurate numerical steady-state one-dimensional solution of the $p-n$ junction. Solid-State-Electronics, *11*, 33 (1968).
4. GUMMEL, H. K.: A self-consistent iterative scheme for one-dimensional steady state transistor calculations. IEEE Transactions on Electron Devices, *ED—11*, 455. (1964).
5. HALL, R. N.: Electron-hole recombination in germanium. Physical Review, *87*, 387 (1952).
6. SHOCKLEY, W.—READ Jr., W. F.: Statistics of the recombination of holes and electrons. Physical Review, *87*, 835 (1952).
7. CAUGHEY, D. M.—THOMAS, E. R.: Carrier mobilities in silicon empirically related to doping and field. Proceedings of the IEEE, *55*, 2192 (1967).
8. CROWELL, C. R.—SZE, S. M.: Current transport in metal-semiconductor barriers. Solid-State Electronics, *9*, 1035 (1966).
9. KENNEDY, D. P.: A mathematical study of space-charge layer capacitance for an abrupt $p-n$ semiconductor junction. Solid-State Electronics, *20*, 311 (1977).

10. HEALD, D. L.—ORDUNG, P. F.—SKALNIK, J. G.—NANSEN, E. N.: Thermodynamic considerations of $p-n$ junction capacitance. Solid-State Electronics, *16*, 1055 (1973).
11. MASSZI, F.—STOLT, L.—TOVE, P. A.—TARNAY, K.: A comparison between the diffusion model and the combined diffusion-thermionic-emission model for M—S junctions by two-carrier numerical computations. Physica Scripta, *24*, 456 (1981).
12. NORDE, H.: A modified forward I—V plot for Schottky diodes with high series resistance. Journal of Applied Physics, *50*, 5052 (1979).

Dr. Ferenc MASSZI 1521 Budapest